LETTERS

Stream denitrification across biomes and its response to anthropogenic nitrate loading

Patrick J. Mulholland[1,2], Ashley M. Helton[3], Geoffrey C. Poole[3,4], Robert O. Hall Jr[5], Stephen K. Hamilton[6], Bruce J. Peterson[7], Jennifer L. Tank[8], Linda R. Ashkenas[9], Lee W. Cooper[2], Clifford N. Dahm[10], Walter K. Dodds[11], Stuart E. G. Findlay[12], Stanley V. Gregory[9], Nancy B. Grimm[13], Sherri L. Johnson[14], William H. McDowell[15], Judy L. Meyer[3], H. Maurice Valett[16], Jackson R. Webster[16], Clay P. Arango[8], Jake J. Beaulieu[8]†, Melody J. Bernot[17], Amy J. Burgin[6], Chelsea L. Crenshaw[10], Laura T. Johnson[8], B. R. Niederlehner[16], Jonathan M. O'Brien[6], Jody D. Potter[15], Richard W. Sheibley[13]†, Daniel J. Sobota[9]† & Suzanne M. Thomas[7]

Anthropogenic addition of bioavailable nitrogen to the biosphere is increasing[1,2] and terrestrial ecosystems are becoming increasingly nitrogen-saturated[3], causing more bioavailable nitrogen to enter groundwater and surface waters[4–6]. Large-scale nitrogen budgets show that an average of about 20–25 per cent of the nitrogen added to the biosphere is exported from rivers to the ocean or inland basins[7,8], indicating that substantial sinks for nitrogen must exist in the landscape[9]. Streams and rivers may themselves be important sinks for bioavailable nitrogen owing to their hydrological connections with terrestrial systems, high rates of biological activity, and streambed sediment environments that favour microbial denitrification[6,10,11]. Here we present data from nitrogen stable isotope tracer experiments across 72 streams and 8 regions representing several biomes. We show that total biotic uptake and denitrification of nitrate increase with stream nitrate concentration, but that the efficiency of biotic uptake and denitrification declines as concentration increases, reducing the proportion of in-stream nitrate that is removed from transport. Our data suggest that the total uptake of nitrate is related to ecosystem photosynthesis and that denitrification is related to ecosystem respiration. In addition, we use a stream network model to demonstrate that excess nitrate in streams elicits a disproportionate increase in the fraction of nitrate that is exported to receiving waters and reduces the relative role of small versus large streams as nitrate sinks.

Biotic nitrogen uptake and denitrification account for nitrogen removal in streams, but a broad synthesis of their relative importance is lacking, in part because of the difficulty of measuring denitrification *in situ* and the lack of comparable data for streams across biomes and land-use conditions. The second Lotic Intersite Nitrogen Experiment (LINX II), a series of ^{15}N tracer additions to 72 streams across multiple biomes and land uses in the conterminous United States and Puerto Rico, provides replicated, *in situ* measurements of total nitrate (NO_3^-) uptake and denitrification. This new data set expands more than tenfold the number and type of streams for which we have reach-scale measurements of denitrification, the primary mechanism by which bioavailable nitrogen is permanently removed from ecosystems.

Streams were small (discharge: 0.2 to 268 $l\,s^{-1}$; median: 18.5 $l\,s^{-1}$) but spanned a wide range of NO_3^- concentration (0.0001 to 21.2 mg N l^{-1}; median: 0.10 mg N l^{-1}) and other environmental conditions such as water velocity, depth and temperature (Supplementary Table 1). Concentrations of NO_3^- were significantly greater in 'agricultural' and 'urban' streams than in 'reference' streams (Fig. 1a), despite substantial variation in the adjacent land use and in-stream conditions within each of these land-use categories.

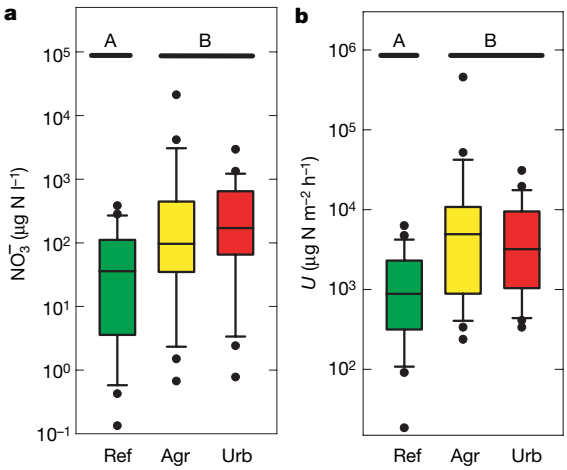

Figure 1 | Observed stream NO_3^- metrics by adjacent land use. **a**, Streamwater NO_3^- concentration. **b**, Total biotic NO_3^- uptake rate per unit area of streambed (U). Box plots display 10th, 25th, 50th, 75th and 90th percentiles, and individual data points outside the 10th and 90th percentiles. Land use had a significant effect on NO_3^- concentration ($P = 0.0055$) and U ($P = 0.0013$) (Kruskal–Wallis test); horizontal bars above plots denote significant differences determined by pairwise comparisons among land-use categories with Bonferroni correction ($\alpha = 0.05$).

[1]Environmental Sciences Division, Oak Ridge National Laboratory, Oak Ridge, Tennessee 37831, USA. [2]Department of Ecology and Evolutionary Biology, University of Tennessee, Knoxville, Tennessee 37996, USA. [3]Odum School of Ecology, University of Georgia, Athens, Georgia 30602, USA. [4]Eco-metrics, Inc., Tucker, Georgia 30084, USA. [5]Department of Zoology and Physiology, University of Wyoming, Laramie, Wyoming 82071, USA. [6]Kellogg Biological Station, Michigan State University, Hickory Corners, Michigan 49060, USA. [7]Ecosystems Center, Marine Biological Laboratory, Woods Hole, Massachusetts 02543, USA. [8]Department of Biological Sciences, University of Notre Dame, Notre Dame, Indiana 46556, USA. [9]Department of Fisheries and Wildlife, Oregon State University, Corvallis, Oregon 97331, USA. [10]Department of Biology, University of New Mexico, Albuquerque, New Mexico 87131, USA. [11]Division of Biology, Kansas State University, Manhattan, Kansas 66506, USA. [12]Institute of Ecosystem Studies, Millbrook, New York 12545, USA. [13]School of Life Sciences, Arizona State University, Tempe, Arizona 85287, USA. [14]Pacific Northwest Research Station, US Forest Service, Corvallis, Oregon 97331, USA. [15]Department of Natural Resources, University of New Hampshire, Durham, New Hampshire 03824, USA. [16]Department of Biological Sciences, Virginia Tech, Blacksburg, Virginia 24061, USA. [17]Department of Biology, Ball State University, Muncie, Indiana 47306, USA. †Present addresses: US Environmental Protection Agency, Cincinnati, Ohio 45268, USA (J.J.B.); US Geological Survey, Tacoma, Washington 98402, USA (R.W.S.); School of Earth and Environmental Sciences, Washington State University, Vancouver Campus, Vancouver, Washington 98686, USA (D.J.S.).

Areal rate of total NO_3^- uptake (U, mass of NO_3^- removed from water per unit area of streambed per unit time) also was greater in agricultural and urban streams (Fig. 1b), suggesting that higher NO_3^- concentration stimulates uptake in these streams. Total uptake velocity of NO_3^- (υ_f, analogous to the average downward velocity at which NO_3^- ions are removed from water, and a measure of uptake efficiency relative to availability[12]) was unrelated to land-use category but declined exponentially with increasing NO_3^- concentration (Fig. 2a). Thus, although excess NO_3^- increased uptake rate per area of streambed, streams became less efficient at removing NO_3^-, indicating that uptake does not increase in parallel with NO_3^- concentration. The value of υ_f also increased with increasing gross primary production rate ($r^2 = 0.204$, $P < 0.0001$), revealing the importance of stream photoautotrophs in NO_3^- removal. Although other research has documented the separate influence of NO_3^- concentration[13,14] and gross primary production rate[15,16] on υ_f within a particular biome, our data reveal their combined influence on NO_3^- removal efficiency, and demonstrate that the loss of efficiency holds across nearly six orders of magnitude in NO_3^- concentration and eight different regions representing several different biomes.

A portion of total NO_3^- uptake in streams can be attributed to denitrification, a microbial process occurring mostly in anoxic zones in the streambed that converts NO_3^- to gaseous forms of nitrogen that are lost to the atmosphere. Our ^{15}N-tracer approach allowed us to directly quantify uptake velocity resulting from denitrification of streamwater NO_3^- (υ_{fden}). The remainder of total NO_3^- uptake represents biotic assimilation and storage in organic (usually particulate) form on the streambed. Some portion of stored nitrogen may be subsequently denitrified via tight spatial coupling of mineralization, nitrification and denitrification in sediments ('coupled denitrification'), which can be important in aquatic systems with NO_3^- concentrations below ~300 μg N l^{-1} (ref. 10). Thus, υ_f describes the upper limit and υ_{fden} the lower limit on rates of biotic NO_3^- removal from stream water.

Like υ_f, υ_{fden} declined exponentially as NO_3^- concentration increased (Fig. 2b), indicating reduced NO_3^- removal efficiency via denitrification with increasing NO_3^- concentration. It also increased with increasing ecosystem respiration rate ($r^2 = 0.318$, $P < 0.0001$), probably because aerobic respiration (that is, ecosystem respiration rate) lowers dissolved oxygen concentration and increases metabolic demand for alternative electron acceptors such as NO_3^-. In addition, ecosystem respiration is likely to be a good surrogate for the availability of labile organic carbon to fuel denitrification. The denitrification fraction of total NO_3^- uptake (ratio of υ_{fden} to υ_f) was highly variable across streams and was unrelated to land use (Fig. 3a), but was positively correlated with ecosystem respiration rate ($r = 0.40$, $P = 0.005$), further supporting the hypothesis that heterotrophic metabolism promotes denitrification[17].

Denitrification accounted for a median of 16% of total NO_3^- uptake across all streams, and exceeded 43% of total uptake in a quarter of our streams. These values are conservative, however, because our measurement method does not account for delayed, coupled denitrification that may occur after NO_3^- is assimilated by biota and remineralized in sediments[10].

Areal denitrification rate (U_{den}), a measure commonly reported in denitrification studies, was greatest in urban streams (Fig. 3b), probably because of high NO_3^- concentration (Fig. 1a). Although our measurements of U_{den} fall within the range observed for other aquatic systems[18], they are lower than other published values for rivers (Fig. 3b), possibly because they do not include coupled denitrification in sediments. However, our measurements of *in situ*, reach-scale denitrification may be more representative of stream ecosystem denitrification than the more commonly used acetylene-block technique in sediment cores[18].

In stream networks, any NO_3^- not removed within a reach passes to the next reach downstream, where it may be subsequently removed. Stream size influences this serial processing in several ways. Small streams can remove NO_3^- efficiently (because of their high ratios of streambed area to water volume) and have a cumulative influence on whole-network removal because they account for most of the stream length within a network[19,20]. By contrast, larger streams are effective NO_3^- sinks owing to longer transport distances and therefore longer water residence times combined with higher nitrogen availability[21,22].

We developed a stream network model of NO_3^- removal, incorporating downstream NO_3^- transport through streams of increasing size and using removal rates that varied with NO_3^- concentration

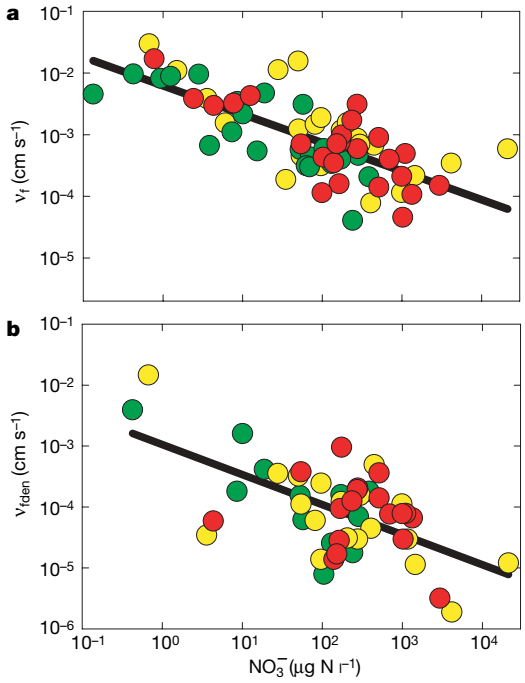

Figure 2 | Relationships between NO_3^- uptake velocity and concentration. **a**, Regression of total NO_3^- uptake velocity (υ_f) on NO_3^- concentration (log $\upsilon_f = -0.462 \times \log[NO_3^-] - 2.206$, $r^2 = 0.532$, $P < 0.0001$). **b**, Regression of denitrification uptake velocity (υ_{fden}) on NO_3^- concentration (log $\upsilon_{fden} = -0.493 \times \log[NO_3^-] - 2.975$, $r^2 = 0.355$, $P < 0.0001$).

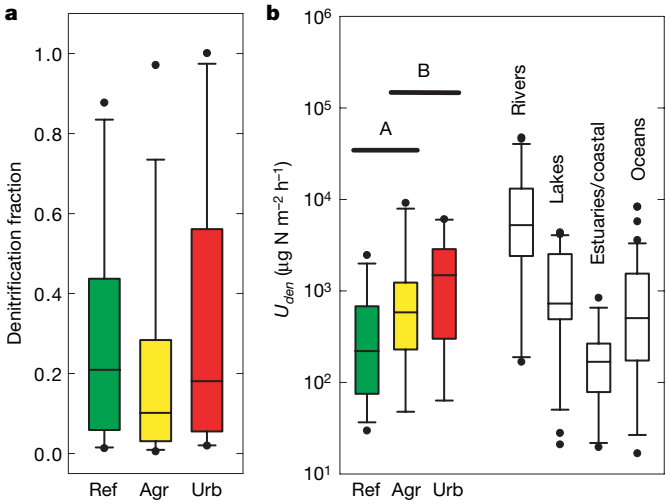

Figure 3 | Observed stream denitrification rates by adjacent land use. **a**, Denitrification as a fraction of total NO_3^- uptake. **b**, Denitrification rate per unit area of streambed (U_{den}), including denitrification rates in other aquatic ecosystems (uncoloured box plots) from a recent compilation[18]. Land use had a significant effect on U_{den} ($P = 0.049$) (Kruskal–Wallis test); horizontal bars above plots denote significant differences determined by pairwise comparisons among land-use categories with Bonferroni correction ($\alpha = 0.05$).

(Fig. 2). We used v_f and v_{fden}, respectively, to model the upper and lower limits on NO_3^- removal. Because our empirically derived rates of denitrification are apt to be conservative (for example, Fig. 3b), so too are the magnitudes of whole-network denitrification predicted by our model. Regardless, the model shows that NO_3^- loading rates may markedly influence the importance of streams as landscape nitrogen sinks. For instance, higher loading rates stimulate NO_3^- uptake and denitrification, but yield an associated disproportionate increase in downstream NO_3^- export to receiving waters (Fig. 4a) as

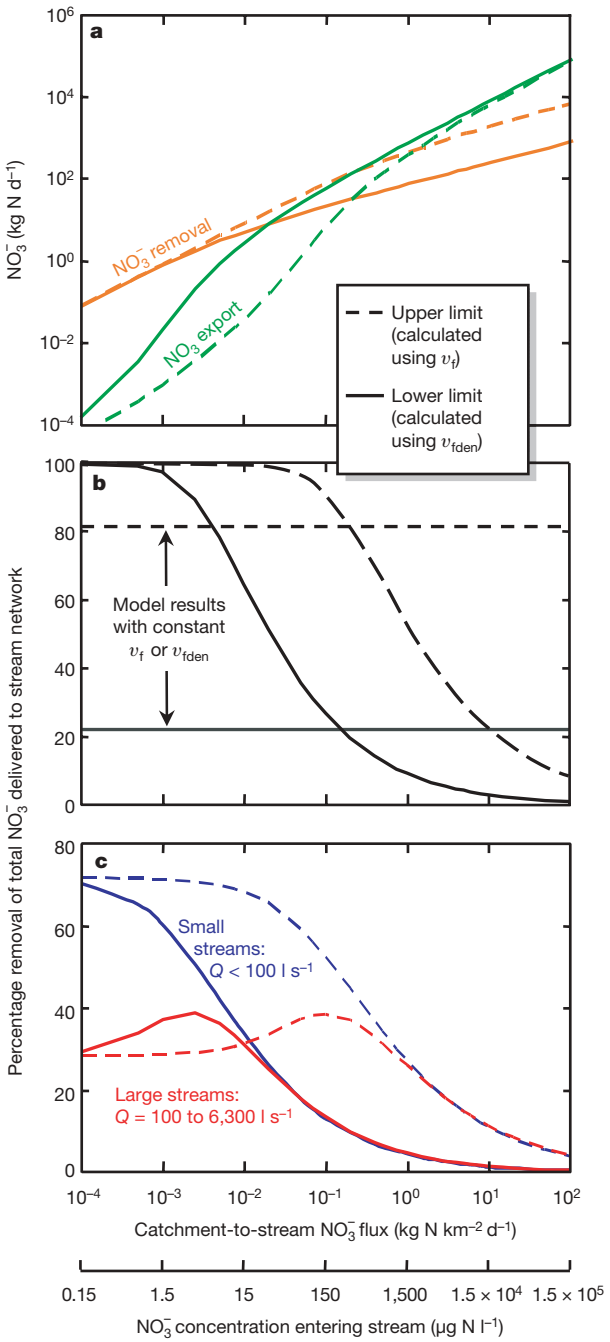

Figure 4 | Simulated upper and lower limits on biotic removal of NO_3^- from stream water within a fifth-order network. **a**, Removal and export of NO_3^- to receiving water bodies versus NO_3^- loading rate (and equivalent concentration in catchment water entering the stream). **b**, Biotic removal expressed as a percentage of total NO_3^- loading to the stream network versus NO_3^- loading rate; curves represent model results when v_f or v_{fden} varies with NO_3^- concentration (according to relationships in Fig. 2), horizontal lines show results using a constant v_f or v_{fden}. **c**, Same as curves in **b**, but divided among 'small' and 'large' streams.

NO_3^- removal efficiency declines (Fig. 4b). The loss of removal efficiency is not addressed by models where v_f is independent of NO_3^- concentration[22], which may yield overly optimistic projections of stream network NO_3^- removal under increasing loading rates (Fig. 4b).

Small and large streams responded differently to simulated increases in NO_3^- loading. The simulated percentage of network NO_3^- load removed in small streams declined as loading increased (Fig. 4c). Unexpectedly, in large streams, simulated percentage removal peaked after NO_3^- loading began to rise, owing to the interaction of two dynamics. Left of the peak, high removal efficiency in small streams yields little downstream NO_3^- transport from small to large streams (Fig. 4a), and therefore, little NO_3^- available for removal in large streams. Thus, percentage removal in large streams increases with NO_3^- loading as downstream transport of NO_3^- increases and large streams are released from NO_3^- limitation. Right of the peak, NO_3^- concentrations in large streams increase to the point where removal efficiency in large streams is lost, and the percentage removal in large streams decreases.

Our modelling results suggest three phases of nitrogen dynamics in stream networks as land-use intensity increases. First, at low nitrogen loading rates, biotic nitrogen removal is high and occurs primarily in smaller streams; removal in larger streams is limited by nitrogen availability. Second, at moderate loading rates, removal efficiency in smaller streams decreases; however, removal in larger streams responds, limiting nitrogen export. Third, at high loading rates, removal becomes ineffective across all stream sizes and the stream network exports virtually all catchment-derived nitrogen. Interestingly, direct anthropogenic NO_3^- loading to large streams (for example, municipal wastewater plants) circumvents the stream network, and therefore may increase the relative role of large versus small streams in network NO_3^- removal. Thus, both small and large streams can be important locations for nitrogen removal, although their relative roles are influenced by uptake efficiency in small streams (which determines downstream transport to large streams) and by the spatial pattern of NO_3^- loading to the stream network.

Across biomes, our empirical data show that NO_3^- removal efficiency decreases and downstream export to receiving water bodies increases as NO_3^- concentration increases. Our modelling expands this finding to explain the response of stream networks as land-use intensity increases. Although our replicated inter-biome experiments add substantial insight to NO_3^- dynamics in streams, we do not address some important considerations (see 'Study Limitations' in Supplementary Information) such as the ultimate fate of nitrogen removed from stream water but not immediately denitrified, variation in removal rates with season and stream discharge, the influence of off-channel and subsurface hydrology associated with floodplains and hyporheic flow paths, and the need for *in situ* empirical observations of nitrogen removal in large streams. These uncertainties prevent comparison of results from short-term, *in situ* experiments with annual stream network nitrogen budgets[7,9,19] and therefore represent critical research needs.

Our findings underscore the management imperative of controlling nitrogen loading to streams and protecting or restoring stream ecosystems to maintain or enhance their nitrogen removal functions. Controlling loading to streams and stream nitrogen export is a proven solution to eutrophication and hypoxia problems in downstream inland and coastal waters[23]. Our findings suggest caution before implementing policies (for example, reliance on intensive agriculture for biofuels production[24]) that may yield massive land conversions and higher nitrogen loads to streams. Associated increases in streamwater NO_3^- concentration may reduce the efficacy of streams as nitrogen sinks, yielding synergistic increases in downstream transport to estuaries and coastal oceans[25–27].

METHODS SUMMARY

We added tracer $^{15}NO_3^-$ using standardized protocols to 72 streams across the contiguous United States and Puerto Rico. Within each of eight regions (Supplementary Fig. 1), three streams were bordered by agricultural lands, three by urban areas, and three by extant vegetation typical of the biome ('reference streams') providing a broad array of stream conditions and land-use intensities. We performed these tracer additions on one date in each stream, generally during the spring or summer. We measured NO_3^- uptake rates for entire stream reaches from measurements of tracer ^{15}N in NO_3^-, N_2 and N_2O downstream from the isotope addition based on the nutrient spiralling approach[12,28,29] and a model of denitrification[30].

Our model of NO_3^- removal from water across a stream network accounted for network topology and downstream changes in channel geometry and discharge. We implemented the model using the topology of a fifth-order stream network, the Little Tennessee River in North Carolina, USA. Simulations included increasing NO_3^- loading rates from the catchment to the network from 0.0001 to 100 kg N km^{-2} d^{-1} (yielding input NO_3^- concentrations from 0.15 μg N l^{-1} to 150 mg N l^{-1}). For each NO_3^- loading rate, we conducted model runs using the median observed υ_f and allowing υ_f to vary with predicted in-stream NO_3^- concentration according to the observed relationship between υ_f and NO_3^- concentration (Fig. 2a). These simulations were repeated using the median observed υ_{fden} and the υ_{fden}–NO_3^- concentration relationship (Fig. 2b). Therefore, model simulations bracket the range of potential network NO_3^- removal (υ_f and υ_{fden} represent upper and lower limits, respectively). To investigate the importance of stream size on network NO_3^- removal, we categorized streams as either 'small' (<100 l s^{-1}, typical of first- and second-order streams) or 'large' (100–6,300 l s^{-1}, typical of third- to fifth-order streams).

Full Methods and any associated references are available in the online version of the paper at www.nature.com/nature.

Received 29 June 2007; accepted 10 January 2008.

1. Vitousek, P. M. *et al.* Human alteration of the global nitrogen cycle: Sources and consequences. *Ecol. Appl.* **7,** 737–750 (1997).
2. Galloway, J. N. *et al.* Nitrogen cycles past, present, and future. *Biogeochemistry* **70,** 153–226 (2004).
3. Aber, J. D. *et al.* Nitrogen saturation in temperate forest ecosystems. *Bioscience* **48,** 921–934 (1998).
4. Bouwman, A. F., Van Drecht, G., Knoop, J. M., Beusen, A. H. W. & Meinardi, C. R. Exploring changes in river nitrogen export to the world's oceans. *Glob. Biogeochem. Cycles* **19,** GB1002, doi:10.1029/2004GB002314 (2005).
5. Johnes, P. J. & Butterfield, D. Landscape, regional and global estimates of nitrogen flux from land to sea: Errors and uncertainties. *Biogeochemistry* **57,** 429–476 (2002).
6. Schlesinger, W. H., Reckhow, K. H. & Bernhardt, E. S. Global change: The nitrogen cycle and rivers. *Water Resource Res.* **42,** W03S06, doi:10.1029/2005WR004300 (2006).
7. Howarth, R. W. *et al.* Riverine inputs of nitrogen to the North Atlantic Ocean: fluxes and human influences. *Biogeochemistry* **35,** 75–139 (1996).
8. Boyer, E. W. *et al.* Riverine nitrogen export from the continents to the coasts. *Glob. Biogeochem. Cycles* **20,** GB1S91, doi:10.1029/2005GB002537 (2006).
9. Van Breemen, N. *et al.* Where did all the nitrogen go? Fate of nitrogen inputs to large watersheds in the northeastern USA. *Biogeochemistry* **57,** 267–293 (2002).
10. Seitzinger, S. P. *et al.* Denitrification across landscapes and waterscapes: a synthesis. *Ecol. Appl.* **16,** 2064–2090 (2006).
11. Hedin, L. O. *et al.* Thermodynamic constraints on nitrogen transformations and other biogeochemical processes at soil–stream interfaces. *Ecology* **79,** 684–703 (1998).
12. Stream Solute Workshop. Concepts and methods for assessing solute dynamics in stream ecosystems. *J. N. Am. Benthol. Soc.* **9,** 95–119 (1990).
13. Dodds, W. K. *et al.* N uptake as a function of concentration in streams. *J. N. Am. Benthol. Soc.* **21,** 206–220 (2002).
14. O'Brien, J. M., Dodds, W. K., Wilson, K. C., Murdock, J. N. & Eichmiller, J. The saturation of N cycling in Central Plains streams: ^{15}N experiments across a broad gradient of nitrate concentrations. *Biogeochemistry*. doi:10.1007/s10533–007–9073–7 (2007).
15. Hall, R. O. & Tank, J. L. Ecosystem metabolism controls nitrogen uptake in streams in Grand Teton National Park, Wyoming. *Limnol. Oceanogr.* **48,** 1120–1128 (2003).
16. Mulholland, P. J. *et al.* Effects of light on NO_3^- uptake in small forested streams: diurnal and day-to-day variations. *J. N. Am. Benthol. Soc.* **25,** 583–595 (2006).
17. Christensen, P. B., Nielsen, L. P., Sørensen, J. & Revsbech, N. P. Denitrification in nitrate-rich streams: Diurnal and seasonal variation related to benthic oxygen metabolism. *Limnol. Oceanogr.* **35,** 640–651 (1990).
18. Piña-Ochoa, E. & Alvarez-Cobelas, M. Denitrification in aquatic environments: A cross-system analysis. *Biogeochemistry* **81,** 111–130 (2006).
19. Alexander, R. B., Smith, R. A. & Schwarz, G. E. Effect of stream channel size on the delivery of nitrogen to the Gulf of Mexico. *Nature* **403,** 758–761 (2000).
20. Peterson, B. J. *et al.* Control of nitrogen export from watersheds by headwater streams. *Science* **292,** 86–90 (2001).
21. Seitzinger, S. P. *et al.* Nitrogen retention in rivers: Model development and application to watersheds in the northeastern USA. *Biogeochemistry* **57,** 199–237 (2002).
22. Wollheim, W. M., Vörösmarty, C. J., Peterson, B. J., Seitzinger, S. P. & Hopkinson, C. S. Relationship between river size and nutrient removal. *Geophys. Res. Lett.* **33,** L06410 (2006).
23. McIsaac, G., David, M. B., Gertner, G. Z. & Goolsby, D. A. Nitrate flux in the Mississippi River. *Nature* **414,** 166–167 (2001).
24. Hill, J., Nelson, E., Tilman, D., Polasky, S. & Tiffany, D. Environmental, economic, and energetic costs and benefits of biodiesel and ethanol biofuels. *Proc. Natl Acad. Sci. USA* **103,** 11206–11210 (2006).
25. Tilman, D., Cassman, K. G., Matson, P. A., Naylor, R. & Polasky, S. Agricultural sustainability and intensive production practices. *Nature* **418,** 671–677 (2002).
26. Foley, J. A. *et al.* Global consequences of land use. *Science* **309,** 570–574 (2005).
27. Beman, J. M., Arrigo, K. R. & Matson, P. A. Agricultural runoff fuels large phytoplankton blooms in vulnerable areas of the ocean. *Nature* **434,** 211–214 (2005).
28. Newbold, J. D., Elwood, J. W., O'Neill, R. V. & Van Winkle, W. Measuring nutrient spiraling in streams. *Can. J. Fish. Aquat. Sci.* **38,** 860–863 (1981).
29. Webster, J. W. & Valett, H. M. in *Methods in Stream Ecology* (eds Hauer, F. R. & Lamberti, G. A.) 169–186 (Elsevier, New York, 2006).
30. Mulholland, P. J. *et al.* Stream denitrification and total nitrate uptake rates measured using a field ^{15}N isotope tracer approach. *Limnol. Oceanogr.* **49,** 809–820 (2004).

Supplementary Information is linked to the online version of the paper at www.nature.com/nature.

Acknowledgements Funding for this research was provided by the National Science Foundation. We thank N. Ostrom for assistance with stable isotope measurements of N_2 and N_2O, and W. Wollheim for initial development of the model that we modified to estimate denitrification rates from field data. We thank M. Mitchell, B. Roberts and E. Bernhardt for their comments on earlier versions of the paper. We thank the NSF LTER network, US Forest Service, National Park Service and many private landowners for permission to conduct experiments on their lands. Partial support to P.J.M. during manuscript preparation was provided by the US Department of Energy, Office of Science, Biological and Environmental Research under contract with UT-Battelle.

Author Contributions P.J.M. coordinated the stream ^{15}N experiments and analysed the compiled experimental data sets. A.M.H. and G.C.P conducted the stream network modelling. P.J.M., A.M.H. and G.C.P. wrote major portions of the manuscript. S.K.H. established sampling protocols and coordinated the ^{15}N analysis of dissolved N_2 samples. Except for A.M.H., all authors listed to J.R.W. were joint project Principal Investigators and contributed to the conceptual and methodological development of the project and analysis of data. Authors listed from C.P.A. to S.M.T. coordinated field experiments and analysed data from one or more biomes. All authors discussed the results and commented on the manuscript.

Author Information Reprints and permissions information is available at www.nature.com/reprints. Correspondence and requests for materials should be addressed to P.J.M. (mulhollandpj@ornl.gov).

METHODS

The second Lotic Intersite Nitrogen Experiment (LINX II) consisted of a series of ^{15}N tracer additions to streams across multiple biomes and land use conditions in the United States and Puerto Rico to provide *in situ*, reach-scale measurements of total nitrate (NO_3^-) uptake and denitrification. Identical protocols were followed at all sites for experimental design and measurement of NO_3^- uptake and denitrification rates, hydraulic and other physical parameters, nutrients, reach-scale rates of metabolism, biomass in various compartments, and stable isotope ratios. We generally followed the methods outlined in a prior ^{15}N-NO_3^- addition study in Walker Branch, Tennessee[30]. Detailed sampling, sample processing and analysis, and calculation protocols for the LINX II study are available at the project website (http://www.biol.vt.edu/faculty/webster/linx/). Selection of study streams, including location and environmental conditions, is presented in Supplementary Fig. 1 and Supplementary Table 1.

Isotope additions. We continuously added a $K^{15}NO_3$ ($\geq$98% ^{15}N) solution to each stream over a 24-h period using a peristaltic or fluid metering pump. The isotope addition was designed to achieve a 20-fold increase in the ^{15}N:^{14}N ratio of streamwater NO_3^-. This level of isotope addition resulted in a small ($\sim$7.5%) increase in the concentration of NO_3^- in stream water. We added NaCl or NaBr to the isotope solution as a conservative tracer to account for downstream dilution due to groundwater input and to measure water velocity and channel hydraulic properties. The isotope additions were started at $\sim$13:00 local time in each stream. Within 1 day of the isotope additions we conducted propane or SF_6 injections to measure air–water gas exchange rates.

Stream sampling and isotope analysis. Stream reaches of 105 to 1,830 m (reach length was dependent on stream size) were sampled at six to ten locations downstream from the isotope addition. We measured tracer ^{15}N flux in NO_3^-, N_2 and N_2O downstream from the addition point after downstream concentrations reached steady state. Samples for ^{15}N were collected once several hours before (to determine natural abundance ^{15}N levels) and twice after the isotope addition commenced: at $\sim$12 h (near midnight) and $\sim$23 h (near noon). We determined ^{15}N-NO_3^- on filtered samples using a sequential reduction and diffusion method[31]. Samples were analysed for ^{15}N on either a Finnigan Delta-S or a Europa 20/20 mass spectrometer in the Mass Spectrometer Laboratory of the Marine Biological Laboratory in Woods Hole, MA (http://ecosystems.mbl.edu/SILAB/aboutlab.html), a Europa Integra mass spectrometer in the Stable Isotope Laboratory of the University of California, Davis (http://stableisotopefacility.ucdavis.edu/) or a ThermoFinnigan DeltaPlus mass spectrometer in the Stable Isotope Laboratory at Kansas State University (http://www.k-state.edu/simsl).

Water samples for ^{15}N-N_2 and ^{15}N-N_2O were collected at each sampling location, equilibrated with helium in 60- or 140-ml syringes, and injected into evacuated vials using underwater transfers of sample and gas to reduce the potential for any air contamination[32]. Gas samples were analysed for ^{15}N by mass spectrometry either using a Europa Hydra Model 20/20 mass spectrometer at the Stable Isotope Laboratory of the University of California, Davis, or a GV Instruments Prism Series II mass spectrometer in the Biogeochemistry Laboratory, Department of Zoology, Michigan State University. The ^{15}N content of all samples was reported in $\delta^{15}N$ notation where $\delta^{15}N = [(R_{SA}/R_{ST}) - 1] \times 1{,}000$, $R = {}^{15}N/{}^{14}N$, and the results are expressed as per mil (‰) deviation of the sample from the standard N_2 in the atmosphere ($\delta^{15}N = 0$‰). All $\delta^{15}N$ values were converted to mole fractions (MF) of ^{15}N ($^{15}N/(^{14}N+{}^{15}N)$), and tracer ^{15}N fluxes were calculated for each sample by multiplying the ^{15}N mole fractions, corrected for natural abundances of ^{15}N by subtracting the average ^{15}N mole fractions for samples collected before the ^{15}N addition, by the concentrations of NO_3^-, N_2, or N_2O in stream water (concentrations of NO_3^- and N_2O were measured, whereas N_2 was taken as the concentration in equilibrium with air at the ambient stream temperature), and stream discharge derived from the measured conservative solute tracer concentrations.

NO_3^- uptake and denitrification rates. We measured NO_3^- uptake rates for entire stream reaches based on the nutrient spiralling approach[28,29] and calculated several metrics describing NO_3^- uptake, including uptake length, uptake velocity and areal uptake rate[12]. Details are provided in the Supplementary Information.

Statistical analysis. To improve normality before parametric statistical analysis all NO_3^- uptake parameters and other variables were log-transformed, with the exception that denitrification fraction was arcsine-square root transformed. Effect of land-use category was determined using analysis of variance (ANOVA) and non-parametric tests on untransformed data. All statistical tests were performed using SAS®, Version 9.1 for Windows (SAS Institute, Inc.).

Stream network model. We developed a simulation model of NO_3^- loading, transport, and biotic uptake within stream networks, and used the model to investigate how NO_3^- removal in stream networks responds to increased loading. The model routes NO_3^- and water from the landscape and through a stream network, and biological uptake removes NO_3^- from the stream water in each reach. Details of model structure and parameterization are presented in the Supplementary Information.

Model runs. The model was implemented for 28 different NO_3^- loading rates to streams under four different υ_f scenarios, for a total of 112 model runs. Water yield per unit catchment area was constant for the stream network across all NO_3^- loading rates and υ_f scenarios. Nitrate loading rate to streams (and, because the water yield was constant, the incoming NO_3^- concentration) was constant across the stream network for each model simulation. Model simulations included systematically increasing NO_3^- loading rates from the catchment to the stream network from 0.0001 to 100 kg N km^{-2} d^{-1} (yielding input NO_3^- concentrations ranging from 0.15 μg N l^{-1} to 150 mg N l^{-1}). For each NO_3^- loading rate, we conducted model runs using a constant υ_f (median observed value) and allowing υ_f to vary with predicted in-stream NO_3^- concentration according to the observed relationship between υ_f and NO_3^- concentration. These simulations were repeated for υ_{fden} (see main text and Supplementary Table 3).

To investigate the relative importance of stream size on NO_3^- removal, we categorized stream reaches as either 'small' ($<$100 l s^{-1}, typical of first- and second-order streams) or 'large' (100–6,300 l s^{-1}, typical of third- to fifth-order streams). Small streams account for 77% of stream length and 50% of streambed surface area across the stream network (see Supplementary Fig. 3). Because we arbitrarily defined distribution of streambed area among 'small' and 'large' categories, the magnitude of NO_3^- removal in small versus large streams (Fig. 4c) is also arbitrary and we focused our analysis on the relative change in the ratio as NO_3^- loading increases.

31. Sigman, D. M. *et al.* Natural abundance-level measurement of the nitrogen isotopic composition of oceanic nitrate: an adaptation of the ammonia diffusion method. *Mar. Chem.* **57**, 227–242 (1997).
32. Hamilton, S. K. & Ostrom, N. E. Measurement of the stable isotope ratio of dissolved N_2 in ^{15}N tracer experiments. *Limnol. Oceanogr. Methods* **5**, 233–240 (2007).